Chirality and wobbling in atomic nuclei (CWAN'23)
July 10-14, 2023, Huizhou (China)

Nuclear chiral rotation induced by superfluidity

Yiping Wang 王一平
YipingWang@pku.edu.cn
Supervisor: Prof. Jie Meng

School of Physics, Peking University

Y. P. Wang, J. Meng, Phys. Lett. B 841 (2023) 137923

Outline

- Introduction
- Theoretical framework
- Numerical details
- Results and discussions
- Summary and Outlook

Nuclear Chirality

- Chiral symmetries exist commonly in nature.

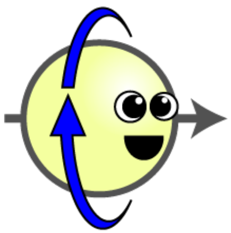

Neutrino

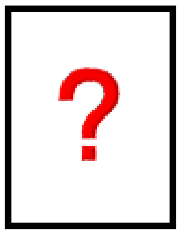

Nucleus

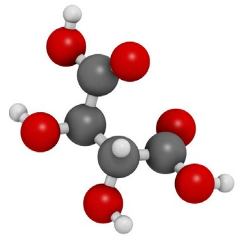

Molecule

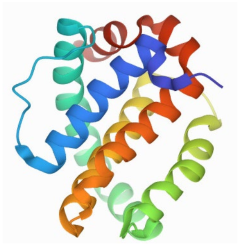

Biomolecule

Organism

Galaxy

- The aplanar rotation of a triaxial nucleus could present chiral geometry.

S. Frauendorf & J. Meng, Nucl. Phys. A. 617 (1997) 131-147

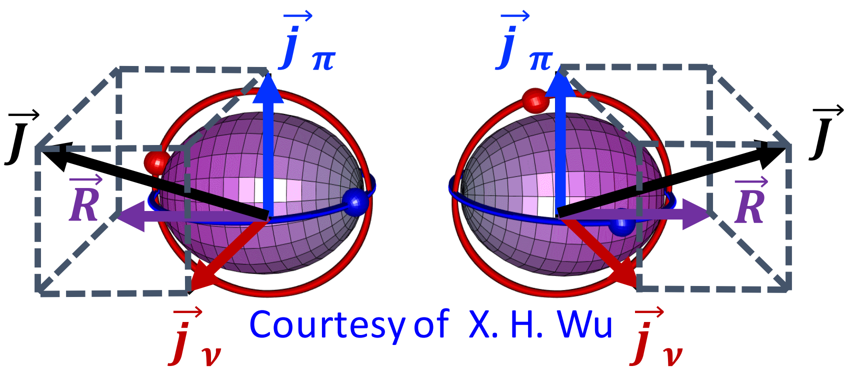

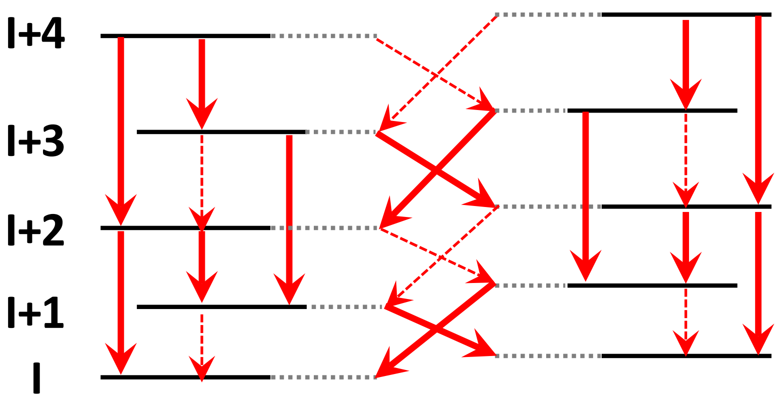

Left-handed $|\mathcal{L}\rangle$ Right-handed $|\mathcal{R}\rangle$

$|I+\rangle = \frac{1}{\sqrt{2}}(|\mathcal{L}\rangle + |\mathcal{R}\rangle)$ $|I-\rangle = \frac{i}{\sqrt{2}}(|\mathcal{L}\rangle - |\mathcal{R}\rangle)$

- Exp. signal： degenerate pair of $\Delta I = 1$ bands, i.e., chiral doublet bands.

Experimental studies

- More than 59 chiral doublet bands in 47 nuclei (including 8 nuclei with MχD) have been reported in the A ~ 80, 100, 130 and 190 mass regions.

B. W. Xiong & Y. Y. Wang, Atomic Data and Nuclear Data Tables 125 (2019) 193–225

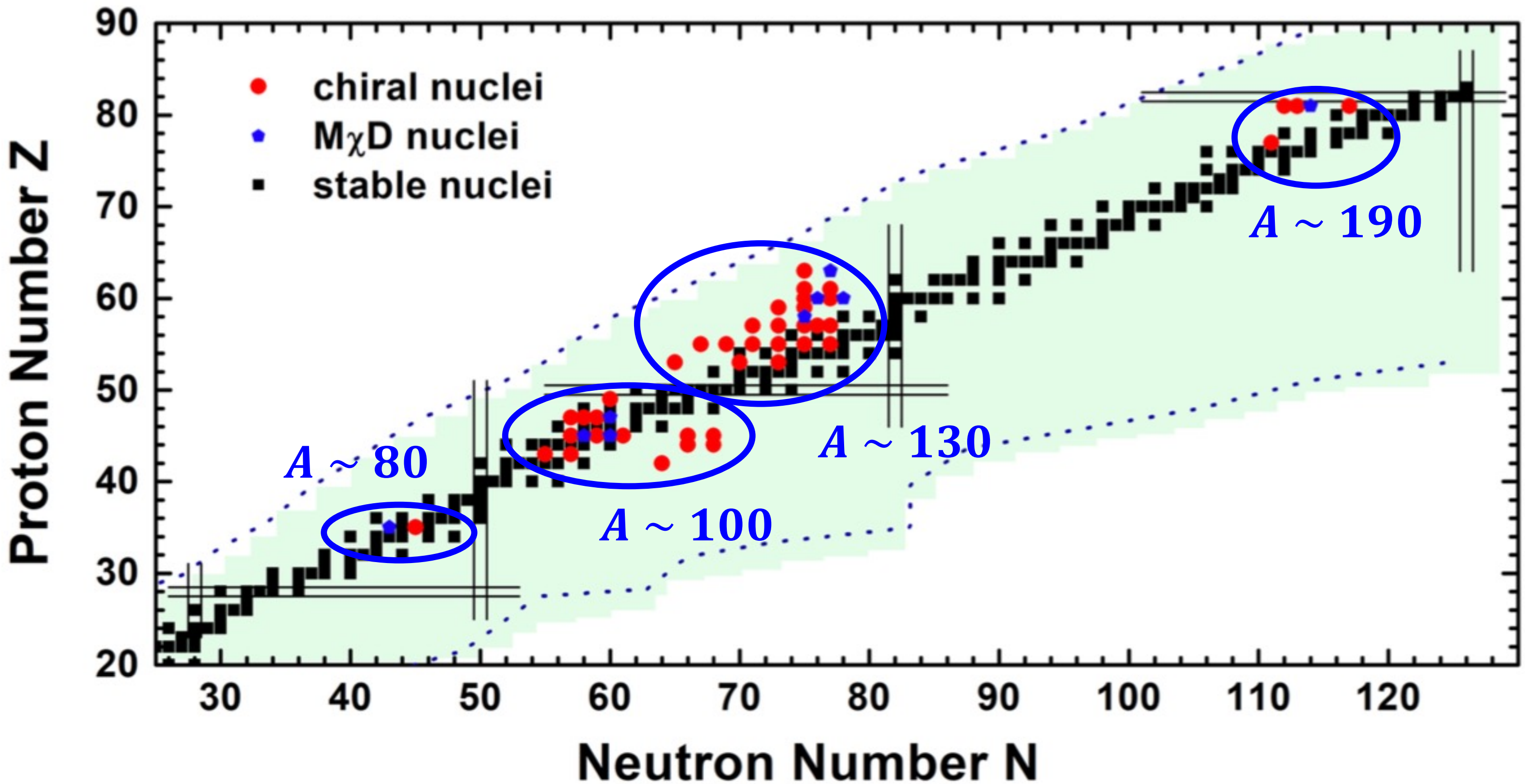

Theoretical studies

- Theoretical approaches for nuclear chirality:
  - Triaxial Particle Rotor Model — Frauendorf&Meng1997NPA; Peng2003PRC;Koike2004PRL; Zhang2007PRC; Qi2009PLB; Chen2018PLB;Wang2019PLB
  - Three-dimensional (3D) cranking Model — Frauendorf&Meng1997NPA; Zhao2017PLB Dimitrov2000PRL; Olbratorwski2004PRL;
  - 3D cranking Model + Random Phase Approximation — Mukhopadhyay2007PRL; Almehed2011PRC
  - 3D cranking Model + Collective Hamiltonian — Chen2013PRC; Chen2016PRC
  - Interacting Boson-fermion-fermion Model — Brant2008PRC
  - Generalized Coherent State Model — Raduta2016JPG
  - Projected Shell Model — Bhat2012PLB, 2014NPA; Chen2017PRC
  - …
- 3D cranking relativistic and nonrelativistic density functional theories: Olbratowski2004PRL; Zhao2017PLB; Peng2020PLB
  - Describe nuclear chirality in a microscopic and self-consistent way.
  - Predict new chiral nuclei.
  - Include important effects (core polarizations, currents, ⋯)

Chiral critical frequency

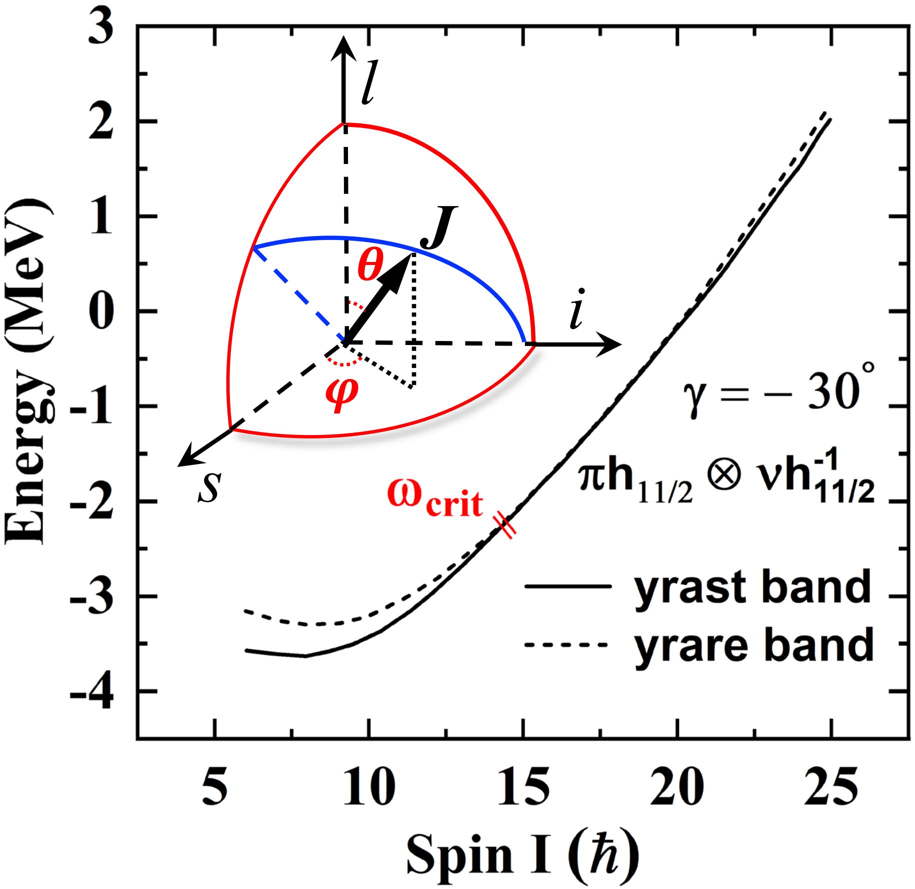

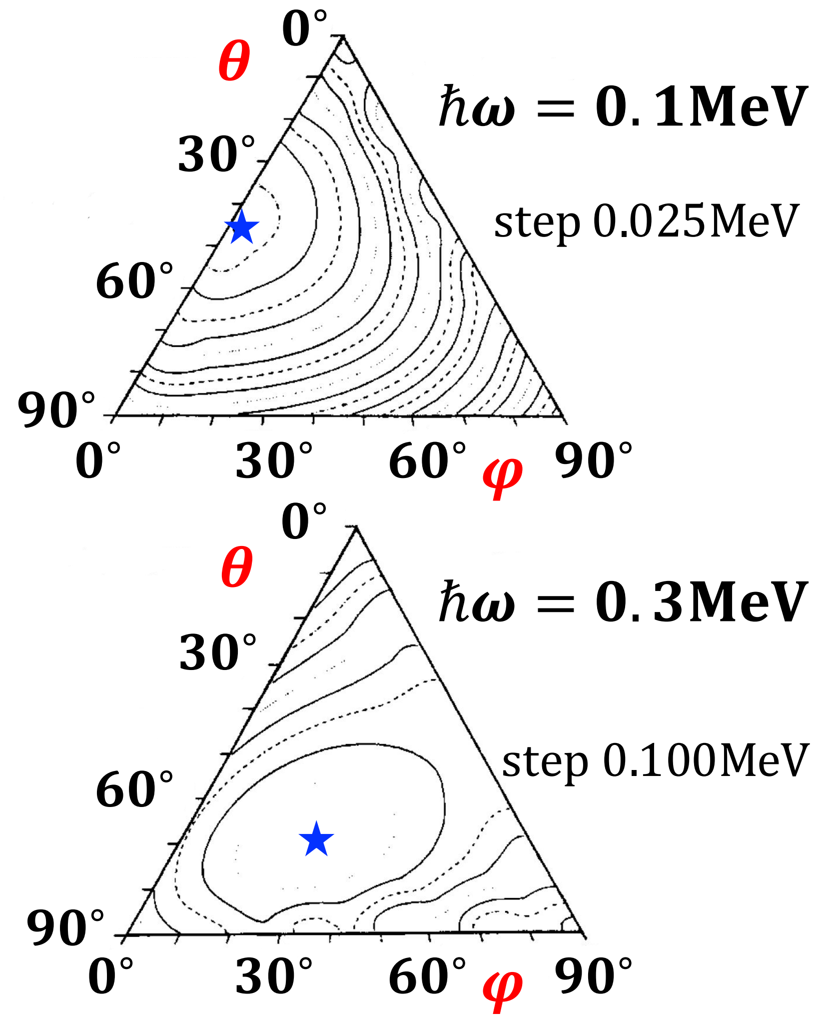

- A transition from planar to aplanar rotation occurs at critical frequency.

S. Frauendorf & J. Meng, Nucl. Phys. A. 617 (1997) 131-147

Nuclear Superfluidity

- Superfluidity plays an important role in nuclei like in condensed matter.
  A. Bohr, et al., Phys. Rev. 110 (1958) 936; S. T. Belyaev, Mat. Fys. Medd. Dan. Vid. Selsk. 31 (1959) 11

- Experimental evidence for nuclear superfluidity:

① Odd-even mass Diff. ② Low-lying Spectra ③ Moments of inertia

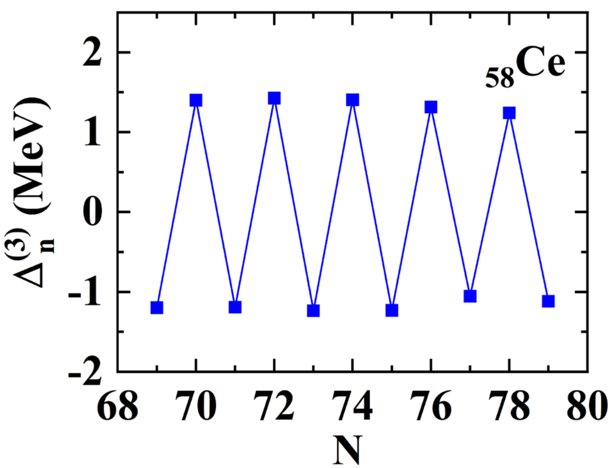

$$\Delta_n^{(3)}(N,Z) = B(N,Z) - \frac{B(N+1,Z)+B(N-1,Z)}{2}$$

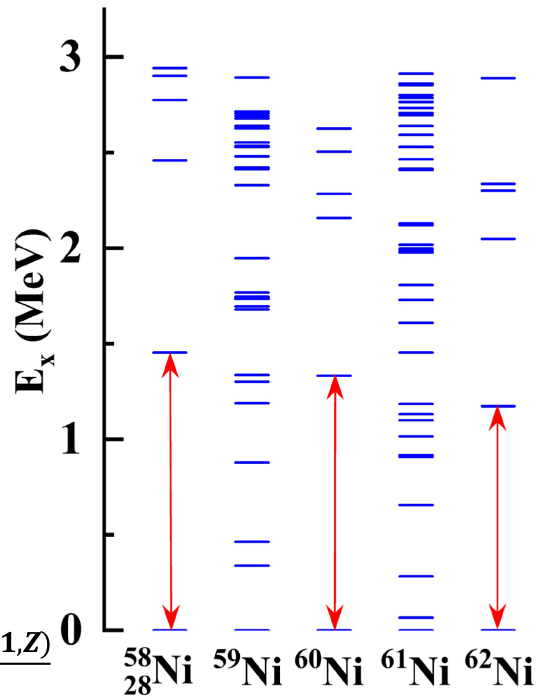

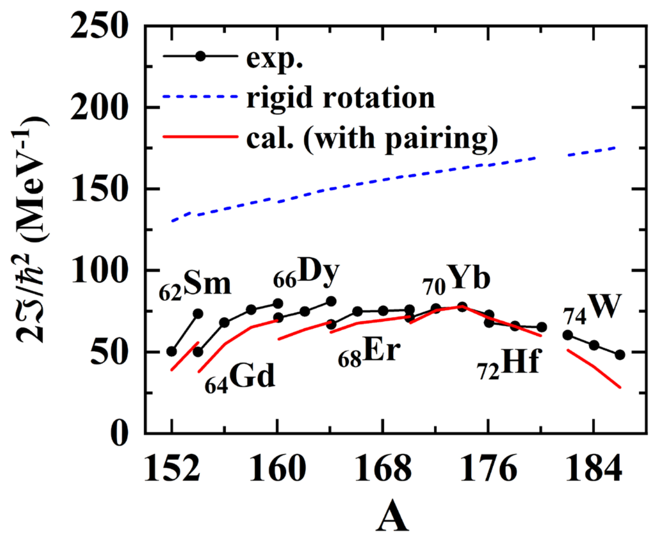

Data from https://www.nndc.bnl.gov/; S. G. Nilsson & O. Prior, Mat. Fys. Medd. Dan. Vid. Selsk. 32 (1961) 16

This work

- Chiral critical frequency has been studied by 3D cranking models with

  - Woods-Saxon potential + Strutinsky method
    V. I. Dimitrov, S. Frauendorf, F. Dönau, Phys. Rev. Lett. 84(25) (2000) 5732–5735
  - Nonrelativistic density functional theories (DFTs)
    P. Olbratowski, et al., Phys. Rev. Lett. 93(5) (2004) 052501
  - Covariant density functional theories (CDFTs)
    P. W. Zhao, Phys. Lett. B 773 (2017) 1; J. Peng, Q.B. Chen, Phys. Lett. B 810 (2020) 135795

  In the DFT calculations, pairing correlations are neglected.

In this work, based on the 3D cranking CDFT,

- A Shell-model-like approach (SLAP) is used to include pairing effects.
- Investigate the chiral doublet bands in $^{135}\mathrm{Nd}$.
- Provide microscopic understanding on the effect of superfluidity on nuclear chiral rotation.

Outline

- Introduction
- Theoretical framework
- Numerical details
- Results and discussions
- Summary and Outlook

Lagrangian density

- The Lagrangian density for the point-coupling version of CDFT:

$$\mathcal{L} = \mathcal{L}^{\rm free} + \mathcal{L}^{\rm 4f} + \mathcal{L}^{\rm hot} + \mathcal{L}^{\rm der} + \mathcal{L}^{\rm em},$$

with

$$\mathcal{L}^{\rm free} = \bar\psi(i\gamma_\mu\partial^\mu - M)\psi,$$

$$\begin{aligned}\mathcal{L}^{\rm 4f} = &-\frac{1}{2}\alpha_S(\bar\psi\psi)(\bar\psi\psi) - \frac{1}{2}\alpha_V(\bar\psi\gamma_\mu\psi)(\bar\psi\gamma^\mu\psi)\\ &-\frac{1}{2}\alpha_{TV}(\bar\psi\vec\tau\gamma_\mu\psi)\cdot(\bar\psi\vec\tau\gamma^\mu\psi) - \frac{1}{2}\alpha_{TS}(\bar\psi\vec\tau\psi)\cdot(\bar\psi\vec\tau\psi),\end{aligned}$$

$$\mathcal{L}^{\rm hot} = -\frac{1}{3}\beta_S(\bar\psi\psi)^3 - \frac{1}{4}\gamma_S(\bar\psi\psi)^4 - \frac{1}{4}\gamma_V\left[(\bar\psi\gamma_\mu\psi)(\bar\psi\gamma^\mu\psi)\right]^2,$$

$$\begin{aligned}\mathcal{L}^{\rm der} = &-\frac{1}{2}\delta_S\partial_\nu(\bar\psi\psi)\partial^\nu(\bar\psi\psi) - \frac{1}{2}\delta_V\partial_\nu(\bar\psi\gamma_\mu\psi)\partial^\nu(\bar\psi\gamma^\mu\psi)\\ &-\frac{1}{2}\delta_{TV}\partial_\nu(\bar\psi\vec\tau\gamma_\mu\psi)\cdot\partial^\nu(\bar\psi\vec\tau\gamma^\mu\psi) - \frac{1}{2}\delta_{TS}\partial_\nu(\bar\psi\vec\tau\psi)\cdot\partial^\nu(\bar\psi\vec\tau\psi),\end{aligned}$$

$$\mathcal{L}^{\rm em} = -\frac{1}{4}F^{\mu\nu}F_{\mu\nu} - e\bar\psi\gamma^\mu\frac{1-\tau_3}{2}\psi A_\mu.$$

J. Meng (Editor). Relativistic Density Functional for Nuclear Structure(2016)

Equation of Motion

- In 3D cranking CDFT, the Lagrangian is transformed to the frame rotating with the uniform velocity $\boldsymbol{\omega}$, corresponding Kohn-Sham equation is

$$\hat{h}_0\psi_k = [\boldsymbol{\alpha}\cdot(-i\boldsymbol{\nabla}-\boldsymbol{V})+\beta(m+S)+V-\boldsymbol{\omega}\cdot\hat{\boldsymbol{J}}]\psi_k = \varepsilon_k\psi_k,$$

- Potentials:

P. W. Zhao, Phys. Lett. B 773 (2017) 1

$$S = \alpha_S\rho_S+\beta_S\rho_S^2+\gamma_S\rho_S^3+\delta_S\Delta\rho_S,$$

$$V = \alpha_V\rho_V+\gamma_V\rho_V^3+\delta_V\Delta\rho_V+\tau_3\alpha_{TV}\rho_{TV}+\tau_3\delta_{TV}\Delta\rho_{TV}+eA^0,$$

$$\boldsymbol{V} = \alpha_V\boldsymbol{j}_V+\gamma_V\left(\boldsymbol{j}_V\right)^3+\delta_V\Delta\boldsymbol{j}_V+\tau_3\alpha_{TV}\boldsymbol{j}_{TV}+\tau_3\delta_{TV}\Delta\boldsymbol{j}_{TV}+e\boldsymbol{A}.$$

- Densities and currents:

$$\rho_S(\boldsymbol{r}) = \sum_{k>0} n_k\bar{\psi}_k(\boldsymbol{r})\psi_k(\boldsymbol{r}), \qquad \rho_c(\boldsymbol{r}) = \sum_{k>0} n_k\psi_k^\dagger(\boldsymbol{r})\frac{1-\tau_3}{2}\psi_k(\boldsymbol{r}),$$

$$\boldsymbol{j}_V(\boldsymbol{r}) = \sum_{k>0} n_k\psi_k^\dagger(\boldsymbol{r})\boldsymbol{\alpha}\psi_k(\boldsymbol{r}), \qquad \rho_V(\boldsymbol{r}) = \sum_{k>0} n_k\psi_k^\dagger(\boldsymbol{r})\psi_k(\boldsymbol{r}),$$

$$\boldsymbol{j}_{TV}(\boldsymbol{r}) = \sum_{k>0} n_k\psi_k^\dagger(\boldsymbol{r})\boldsymbol{\alpha}\tau_3\psi_k(\boldsymbol{r}), \qquad \rho_{TV}(\boldsymbol{r}) = \sum_{k>0} n_k\psi_k^\dagger(\boldsymbol{r})\tau_3\psi_k(\boldsymbol{r}).$$

Solve the equation of motion in 3DHO bases

- The Kohn-Sham equation can be solved by expanding the spinors in the 3D Cartesian harmonic oscillator (3DHO) bases

$$\begin{cases} \Phi_{\underline{\xi}}(\boldsymbol{r},s) = \phi_{n_x}(x)\phi_{n_y}(y)\phi_{n_z}(z)\dfrac{i^{n_y}}{\sqrt{2}}\begin{pmatrix} 1 \\ (-1)^{n_x+1} \end{pmatrix}, & \text{with } \underline{\xi} = |n_x, n_y, n_z, +i\rangle\,, \\ \Phi_{\bar{\xi}}(\boldsymbol{r},s) = \phi_{n_x}(x)\phi_{n_y}(y)\phi_{n_z}(z)\dfrac{(-i)^{n_y}}{\sqrt{2}}\begin{pmatrix} (-1)^{n_x+1} \\ -1 \end{pmatrix}, & \text{with } \bar{\xi} = |n_x, n_y, n_z, -i\rangle\,, \end{cases}$$

J. Peng, et al., Phy. Rev. C 78 (2008) 024313

- For the time-reversal operator $\hat{\mathcal{T}} = i\sigma_y\hat{\mathcal{K}}$,

$$\hat{\mathcal{T}}\Phi_{\underline{\xi}}(\boldsymbol{r},s) = \Phi_{\bar{\xi}}(\boldsymbol{r},s)\,, \qquad \hat{\mathcal{T}}\Phi_{\bar{\xi}}(\boldsymbol{r},s) = -\Phi_{\underline{\xi}}(\boldsymbol{r},s)\,.$$

- Diagonalizing $\hat{h}_0$ in the 3DHO bases, ψ_k is obtained,

$$\psi_k = \begin{pmatrix} \sum_{\underline{\xi}} D^f_{\underline{\xi}k}\Phi_{\underline{\xi}} + \sum_{\bar{\xi}} D^f_{\bar{\xi}k}\Phi_{\bar{\xi}} \\ \sum_{\underline{\tilde{\xi}}} D^g_{\underline{\tilde{\xi}}k}\Phi_{\underline{\tilde{\xi}}} + \sum_{\bar{\tilde{\xi}}} D^g_{\bar{\tilde{\xi}}k}\Phi_{\bar{\tilde{\xi}}} \end{pmatrix},$$

where $D^f_{\underline{\xi}k}$ $(D^g_{\underline{\tilde{\xi}}k})$ and $D^f_{\bar{\xi}k}$ $(D^g_{\bar{\tilde{\xi}}k})$ are the expansion coefficients.

Cranking Many-body Hamiltonian

- Based on ψ_k obtained in 3D cranking CDFT, SLAP is applied to take into account the pairing correlations.
- The idea of SLAP is to diagonalize the Hamiltonian in a properly truncated many-particle configuration space with exact particle number.

J. Y. Zeng, T. S. Cheng, NPA 405 (1983) 1–28; J. Meng, et al., Front. Phys. China 1 (2006) 38–46

- The cranking many-body Hamiltonian $\hat{H} = \hat{H}_0 + \hat{H}_{\text{pair}}$.
  - One-body Hamiltonian: $\hat{H}_0 = \sum \hat{h}_0$
  - Two-body Hamiltonian: $\hat{H}_{\text{pair}} = -G \sum\limits_{\underline{\xi},\underline{\eta}>0} \hat{\beta}^\dagger_{\underline{\xi}} \hat{\beta}^\dagger_{\bar{\xi}} \hat{\beta}_{\bar{\eta}} \hat{\beta}_{\underline{\eta}},$

    $\hat{\beta}^\dagger_{\underline{\xi}(\bar{\xi})}$ ($\hat{\beta}_{\underline{\eta}(\bar{\eta})}$) are the creation (annihilation) operators for the 3DHO bases.
  - $\hat{H}_{\text{pair}}$ can be rewritten in the cranking single-particle bases as

$$\begin{aligned}\hat{H}_{\text{pair}} = -G \sum_{k_1 k_2 k_3 k_4} \Big(& \sum_{\underline{\xi},\underline{\eta}>0} D^{f*}_{\underline{\xi}k_1} D^{f*}_{\bar{\xi}k_2} D^{f}_{\bar{\eta}k_4} D^{f}_{\underline{\eta}k_3} + \sum_{\underline{\xi},\tilde{\eta}>0} D^{f*}_{\underline{\xi}k_1} D^{f*}_{\bar{\xi}k_2} D^{g}_{\bar{\tilde{\eta}}k_4} D^{g}_{\underline{\tilde{\eta}}k_3} \\ & + \sum_{\tilde{\xi},\underline{\eta}>0} D^{g*}_{\underline{\tilde{\xi}}k_1} D^{g*}_{\bar{\tilde{\xi}}k_2} D^{f}_{\bar{\eta}k_4} D^{f}_{\underline{\eta}k_3} + \sum_{\tilde{\xi},\tilde{\eta}>0} D^{g*}_{\underline{\tilde{\xi}}k_1} D^{g*}_{\bar{\tilde{\xi}}k_2} D^{g}_{\bar{\tilde{\eta}}k_4} D^{g}_{\underline{\tilde{\eta}}k_3} \Big) \hat{b}^\dagger_{k_1} \hat{b}^\dagger_{k_2} \hat{b}_{k_4} \hat{b}_{k_3}.\end{aligned}$$

Many-particle Configuration and Eigenstates

- The many-particle configuration (MPC) for the A-particle system is

$$|i\rangle \equiv |k_1 k_2 \cdots k_A\rangle = \hat{b}^\dagger_{k_1} \hat{b}^\dagger_{k_2} \cdots \hat{b}^\dagger_{k_A} |0\rangle.$$

- Diagonalizing $\hat{H}$ in the MPC space, the eigenstates are obtained,

$$\Psi = \sum_i C_i |i\rangle,$$

with the expanding coefficients C_i.

- Occupation probability n_k for the single-particle state ψ_k :

$$n_k = \sum_i |C_i|^2 P_i^k, \quad P_i^k = \begin{cases} 1, & \psi_k \text{ is occupied in MPC } |i\rangle, \\ 0, & \text{otherwise.} \end{cases}$$

The occupation probabilities are used to calculate the densities and currents, which are iterated back to the equation of motion.

Self-consistent calculation

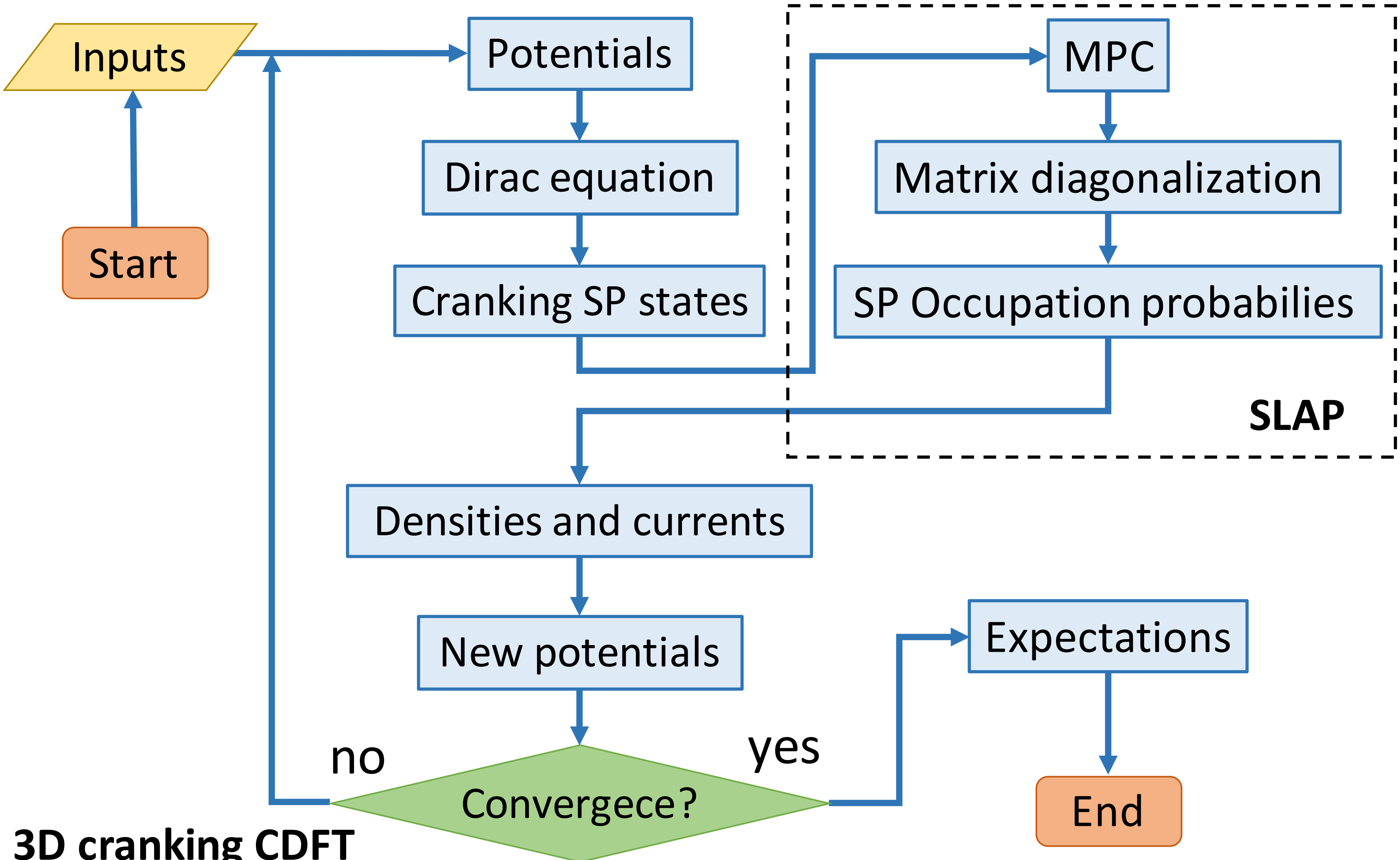

Observables and Expectations

- Angular momentum components:

$$J_q = \langle \Psi | \hat{J}_q | \Psi \rangle, \quad q = x, y, z.$$

And the quantized momentum I is obtained from $\langle \hat{\boldsymbol{J}} \rangle^2 = I(I+1)$.

- Quadrupole moments:

$$Q_{20} = \sqrt{\frac{5}{16\pi}} \langle 3z^2 - r^2 \rangle, \quad Q_{22} = \sqrt{\frac{15}{32\pi}} \langle x^2 - y^2 \rangle.$$

- Magnetic moment:

$$\boldsymbol{\mu} = \sum_{k>0} n_k \int d^3 r \left[\frac{mc^2}{\hbar c} q \psi_k^\dagger \boldsymbol{r} \times \boldsymbol{\alpha} \psi_k + \kappa \psi_k^\dagger \beta \boldsymbol{\Sigma} \psi_k \right]$$

with $q = 1$, $\kappa = 1.793$ for protons, $q = 0, \kappa = -1.913$ for neutons.

- Electromagnetic transition probabilities:

$$B(M1) = \frac{3}{8\pi} \left\{ \left[-\mu_z \sin\theta + \cos\theta \left(\mu_x \cos\varphi + \mu_y \sin\varphi \right) \right]^2 + \left(\mu_y \cos\varphi - \mu_x \sin\varphi \right)^2 \right\},$$

$$B(E2) = \frac{3}{8} \left[Q_{20}^p \sin^2\theta + \sqrt{\frac{2}{3}} Q_{22}^p \left(1 + \cos^2\theta \right) \cos 2\varphi \right]^2 + \left(Q_{22}^p \cos\theta \sin 2\varphi \right)^2.$$

Outline

- Introduction
- Theoretical framework
- Numerical details
- Results and discussions
- Summary

Numerical Details

- Nucleus : $^{135}\mathrm{Nd}$
- Configuration : $\pi h_{11/2}^{2} \otimes \nu h_{11/2}^{-1}$
- Relativistic density functional : PC-PK1
  P. W. Zhao, *et al*., Phys. Rev. C, 82 (2010) 054319
- Major shells of the 3DHO bases: 10
- MPC space dimension: 1000
- Pairing strengths: $G_{\mathrm{n}} = 0.55$ MeV; $G_{\mathrm{p}} = 0.60$ MeV

	Exp.	Cal.
$\Delta_{\mathrm{n}}^{(3)}(\mathrm{MeV})$	1.21	1.20
$\Delta_{\mathrm{p}}^{(3)}(\mathrm{MeV})$	1.37	1.38

Outline

- Introduction
- Theoretical framework
- Numerical details
- Results and discussions
- Summary and Outlook

$I - \omega$ relation & B(M1) & B(E2)

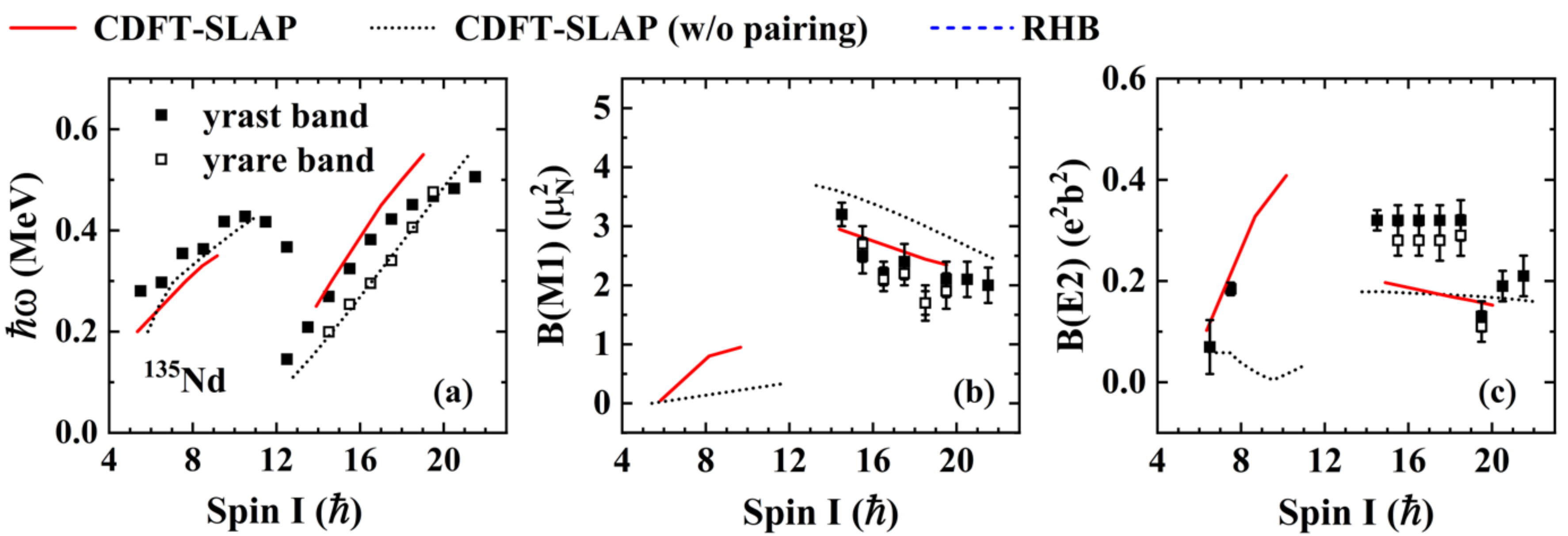

Data from S. Zhu, et al., PRL 91 (2003) 132501; S. Mukhopadhyay, et al., PRL 99 (2007) 172501

- Configuration: $\nu h_{11/2}^{-1}$ (1-qp band) ; $\pi h_{11/2}^{2} \otimes \nu h_{11/2}^{-1}$ (3-qp band)
- Better agreements with the data are achieved with pairing:
  - Moment of inertia I/ω for the 3-qp band reduced
  - $B(M1)$ for the 3-qp band suppressed
  - $B(E2)$ for the 1-qp band enhanced

Chiral critical frequency

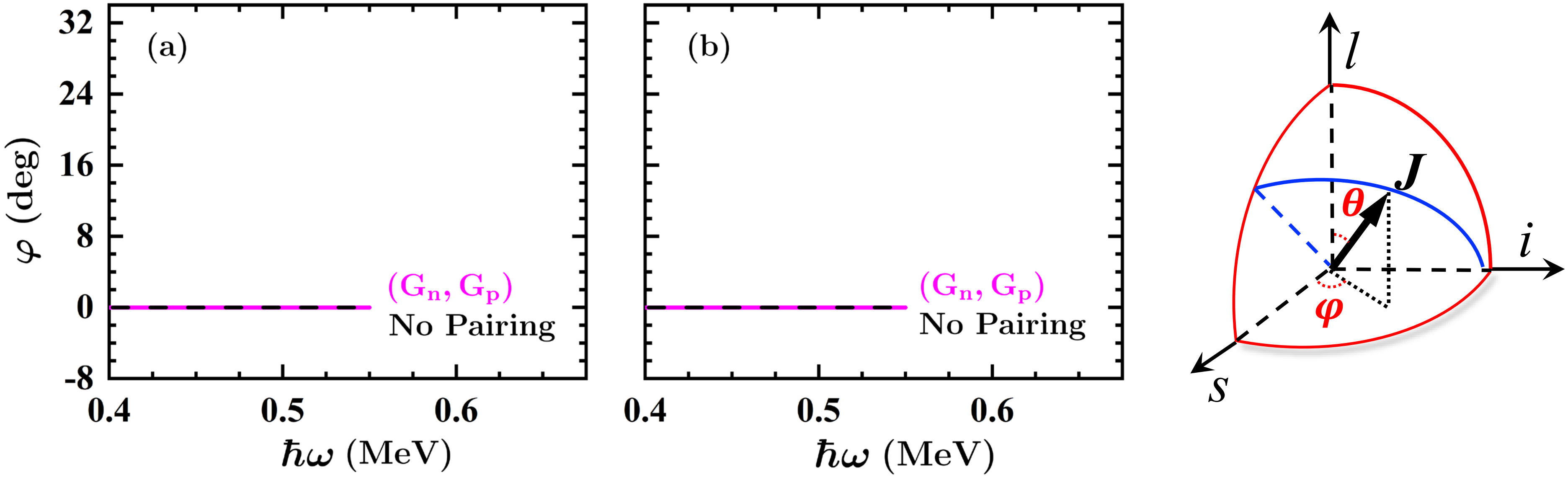

- Without pairing, the angle φ is always zero with the rotation.
- With the pairing strengths $(\mathrm{G_n}, \mathrm{G_p})$, φ still remains to be zero.
- There is no chiral rotation up to $\hbar\omega = 0.55$MeV.

Chiral critical frequency

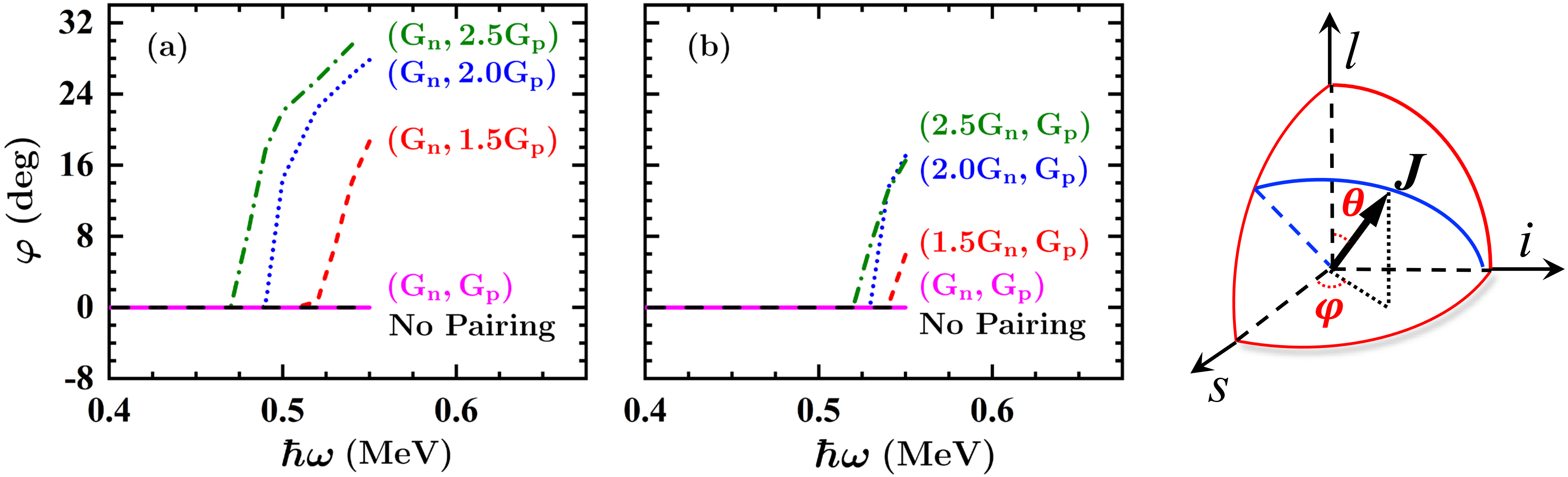

- With the pairing strengths enhanced, nonzero value of φ appears.
- The pairing correlations induce the early appearance of chiral rotation.
- The critical frequency is more sensitive to the proton pairing than neutron for the 3-qp band in ^{135}Nd.

Moments of inertia (MOIs)

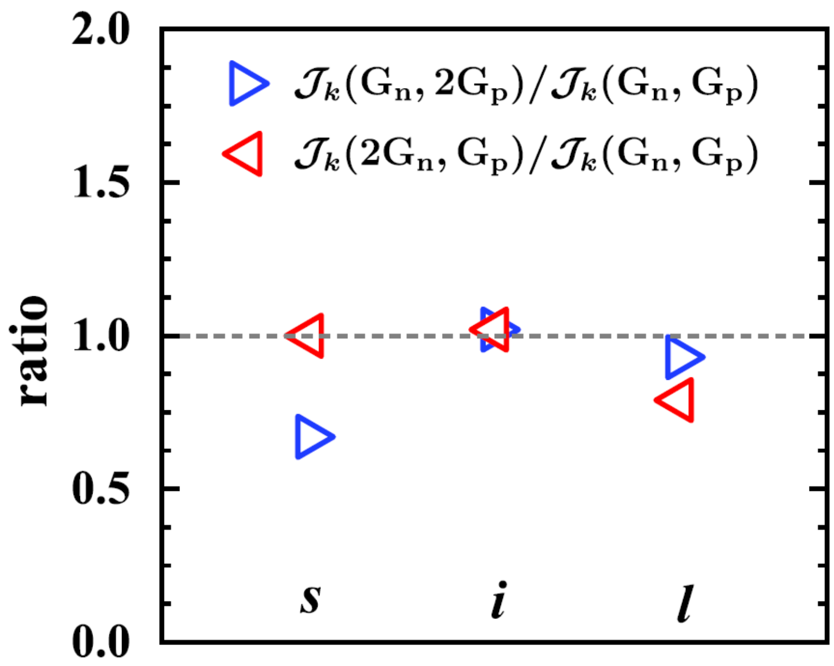

Moments of inertia (MOIs)

$$\mathcal{J}_k = \frac{dJ_k}{d\omega_k}, \qquad k = s, i, l$$

- $(\mathrm{G_n}, \mathrm{G_p}) \to (\mathrm{G_n}, 2\mathrm{G_p})$, $\mathcal{J}_s$ is suppressed, $\mathcal{J}_i$ and $\mathcal{J}_l$ are almost unchanged.
- $(\mathrm{G_n}, \mathrm{G_p}) \to (2\mathrm{G_n}, \mathrm{G_p})$, $\mathcal{J}_l$ is suppressed, $\mathcal{J}_i$ and $\mathcal{J}_s$ are almost unchanged.
- The suppression of $\mathcal{J}_s$ or $\mathcal{J}_l$ results in the enhanced preference of collective rotation along *i* axis, thus early appearance of chiral rotation.

Quadrupole and Triaxial deformation

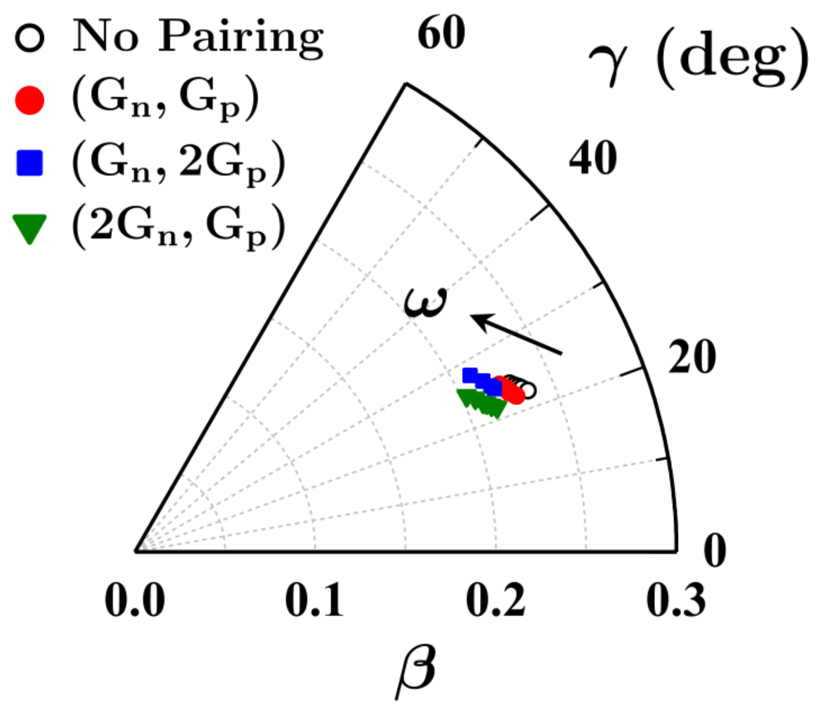

- The pairing effect on deformation is negligible.
- The MOIs for the collective rotation remain almost unchanged.
- The suppression of $\mathcal{J}_s/\mathcal{J}_l$ is due to the reduction of the particle/hole alignments along the s/l axis by the proton/neutron pairing.

Outline

- Introduction
- Theoretical framework
- Numerical details
- Results and discussions
- Summary and Outlook

Summary and Outlook

- Based on the 3D cranking CDFT, the SLAP with exact particle number conservation is applied to take into account the pairing correlations.
- The chiral doublet bands built on $\pi h^{2}_{11/2} \otimes \nu h^{-1}_{11/2}$ in $^{135}\mathrm{Nd}$ is investigated.
  - The $I-\omega$ relation, $B(M1)$ and $B(E2)$ transitions are well reproduced.
- Microscopic understanding on the influence of the pairing correlations on the nuclear chiral rotation is provided:
  - Superfluidity reduces the critical frequency and makes chiral rotation easier.
  - The particle/hole alignments along the s/l axis are reduce by pairing.
  - The preference of the collective rotation along the i axis is enhanced.
- Outlook: Systematic study of chiral doublet bands, wobbling, $\cdots$

Thank you for your attention!